

Hydrological Modeling of Large River Basin using Soil Moisture Accounting Model and Monte Carlo Simulation

Gauri Patil* and Rajesh Kherde

DY Patil University Ambi, Pune Maharashtra 410506, India

(*Corresponding author's e-mail: gauri.patil2310@gmail.com)

Received: 8 November 2023, Revised: 27 December 2023, Accepted: 3 January 2024, Published: 30 March 2024

Abstract

This description outlines a Geographic Information System (GIS)-based rainfall-runoff model that simulates the flow of water in a river basin. The model operates on a daily time step and consists of 4 non-linear storage components: Interception, soil moisture, channel, and groundwater. It employs (SCS) Unit Hydrograph model to determine unit hydrograph ordinates. The model replicates the movement and storage of water in various parts of the basin, including vegetation, the soil surface, the soil profile, and groundwater layers. To address uncertainty, a Monte Carlo simulation feature is integrated into the model. Monte Carlo Simulation involves predicting outcomes by generating numerous iterations using estimated ranges of values for variables with inherent uncertainty. This feature generates required number of sample sets with random parameter values. The model is run for all these realizations during a calibration period, and performance metrics like NSE are calculated for each calibration year to assess prediction uncertainty, model parameter weights are computed by normalizing the corresponding likelihood values. These weights sum up to one and represent the probabilistic distribution of predicted variables, illustrating the impact of structural and parameter errors on model predictions. A sensitivity analysis reveals that the Muskingum constants K and X have the greatest influence on model performance, while parameters Φ_{gw} , Φ_{sw} , Φ_{fc} , and Φ_{pc} have a minimal effect on the model's performance. The outcomes presented in the findings indicate that the Soil moisture accounting Model successfully forecasted peak discharge by leveraging the existing historical data. The accuracy of both volume and timing in the predictions suggests the model's appropriateness for the examined catchments.

Keywords: SMA model, Monte Carlo Simulation, Optimization, Uncertainty analysis, Sensitivity analysis

Introduction

General

Water plays a crucial role as a catalyst for economic and social progress, serving as a fundamental component essential for maintaining the balance and health of the natural environment [1]. Certainly, water is essential for sustaining life, but it can also present hazards and perils, particularly in the context of natural disasters like excessive rainfall and flooding [2-4]. The water cycle entails the perpetual movement of water within the Earth's atmospheric system. While precipitation and runoff are observable elements of this hydrologic cycle, there are other imperceptible components such as infiltration, evapotranspiration, percolation, groundwater recharge, and discharge. Although the basic representation of water exchange between these components is straightforward, accurately quantifying the intricate interactions among them proves. The quantity of surface runoff is impacted by factors such as soil characteristics, land cover, hill slope, vegetation, and storm attributes, including the duration, amount, and intensity of rainfall [5,6]. Given that surface runoff is the primary source of detrimental impacts on streams, it is imperative to model and understand runoff as a crucial step in preventing and effectively managing its adverse effects [7,8]. In an era marked by the rising scarcity of natural resources and widespread impacts of human activities, it is essential to utilize the most effective tools for environmental characterization, impact prediction, and the formulation of plans to mitigate adverse effects and promote sustainability [9]. **Figure 1** given below Represents hydrological processes of a basin [10].

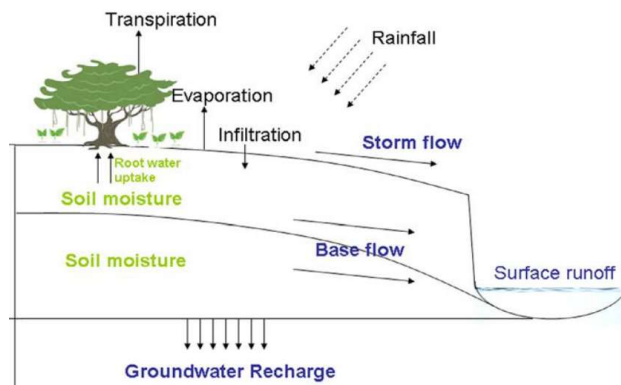


Figure 1 Representation of hydrological processes.

Modeling plays a pivotal role in comprehending the hydrological dynamics of watersheds [11,12]. It aids in predicting forthcoming conditions, endorsing effective watershed management practices, and facilitating well-informed decision-making for sustainable water resource management [13,14]. The emphasis lies in rainfall-runoff modeling, exploring how the conversion of rainfall into runoff can be simulated using various mathematical tools that articulate runoff generation processes for large river basin (Area > 250 km²) [15,16]. The latest advancements in geographic information system (GIS) techniques have significantly improved the capacity to manage extensive databases that detail the variability's in land surface characteristics [17,18].

In the present research, computer-based software, the Soil Moisture Accounting (SMA) model, was devised in conjunction with Geographic Information System (GIS) for the Wainganga River basin, which is part of the Godavari Basin in India. The model operates on a daily time step and integrates a framework into a fundamental rainfall-runoff model. This framework combines the loss method and Muskingum routing for hydrological modeling, complemented by Monte Carlo simulation. Monte Carlo Simulation involves predicting outcomes by generating numerous iterations using estimated ranges of values for variables with inherent uncertainty. Instead of relying on fixed input values, this method constructs a model by employing probability distributions like uniform or normal distributions. The simulation iteratively recalculates results, each time utilizing a different set of random numbers within the specified minimum and maximum values. This method is advantageous as compared to other traditional method due to Enhance the process of making decisions and address intricate issues with simplicity. The process is typically repeated 10,000 of times in a Monte Carlo experiment, generating a multitude of probable outcomes. Data-driven models identify the optimal relationship by analyzing input data series and corresponding output, enabling the modeling of the runoff process. The Soil Moisture Accounting (SMA) method emulates the flow and retention of water within the soil profile, encompassing multiple groundwater layers [19]. In a hydrological model, SMA extends beyond solely estimating soil moisture; it fundamentally serves as an inclusive framework that incorporates surface runoff and evapotranspiration.

Materials and methods

The methodology can be divided into various major tasks: 1) Obtaining the Geographic locations of the catchment area; 2) Data collection of Meteorological input, topography data, observed stream and Curve numbers for basin; 3) Delineation of water shed including DEM processing, delineating streams and watershed characteristics, terrain processing, and basin processing; 4) Determination of canopy coverage using GIS; 5) Determination of soil hydraulic parameters; 6) Development of soil moisture accounting model 7) Parameter optimization, Sensitivity And Uncertainty analysis Of Model Parameter.

Study area

The model is applied to Wainganga river basin. **Figure 2(a)** highlights the river basin of India, specifically focusing on the Godavari river basin (312,800 km²) situated in the Deccan plateau [20,21].

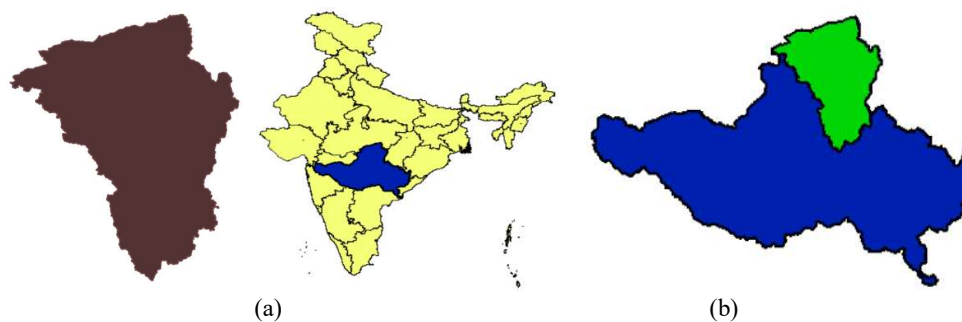


Figure 2 (a) Location Map of Godavari River basin and (b) Wainganga Basin.

Figure 2(b) represent Wainganga basin (51,550.60 km²), which serves as a sub-catchment of the Godavari basin. The basin's topographical shape, depicted in **Figure 2(b)**, resembles a top shape and is positioned between longitude 78°0'-80°45' E and latitudes 19°41'-22°50' N. The origin of the Wainganga is in Mahadeo hill in Seoni, Madhya Pradesh, covering areas in the states of Maharashtra and Madhya Pradesh. The whole basin drains at the outlet named Ashti situated on the Wainganga. The elevation of the catchment varies from 130 to 1,250 m above MSL.

Data collection

Wainganga basin is delineated by using the shuttle radar topography mission (SRTM) dataset with digital elevation model (DEM) of 30×30 m² spatial resolution from USGS Earth Explorer. Area covered by basin, Sub basin area, stream length, slope was calculated through digitized map [22]. Meteorological input data was obtained from Meteorological Department (IMD) for a resolution of 0.25×0.25 ° (imd.gov.in). Total 93 stations rainfall data was collected for a period of 2001 - 2017. The observed stream flows were collected from India Water Resources Information System (India WRIS, indiawris.gov.in) for period of 2001 - 2017. The observed discharge is collected from HDUG Nasik. H.D.U.G. (mahahp.gov.in).

Watershed delineation

The Hydrologic Engineering Center (HEC) introduced HEC-HMS, a computer application developed as part of the Research and Development Program of the U.S. Army Corps of Engineers (USACE). Its initial release occurred in 1992. HEC-HMS is specifically crafted to model precipitation-runoff processes in dendritic watershed systems. Its versatility allows for application across diverse geographic areas and addresses a broad spectrum of hydrological issues [23,24]. The final program release, named Version 4.0, featured an enhanced GIS component. In this study, the HEC-HMS 4.10 model was employed, comprising 4 key components: Basin Model Manager, Terrain Data Manager, Meteorological Model Manager, and Control Specification Manager, along with a Time-Series Data Manager. DEM Tiles obtained from USGS are combined using ArcGIS to generate a single Digital Elevation Model (DEM), which is then exported to HEC-HMS. The creation of a basin model is facilitated through the Basin Model Manager.

In the current investigation, the Ashti station serves as the designated break point, with the assumption that the entire basin directs its drainage toward this location. The model is then delineated to generate the basin model, and **Figure 3** illustrates the diverse stages showing processing of the DEM into a delineated watershed.

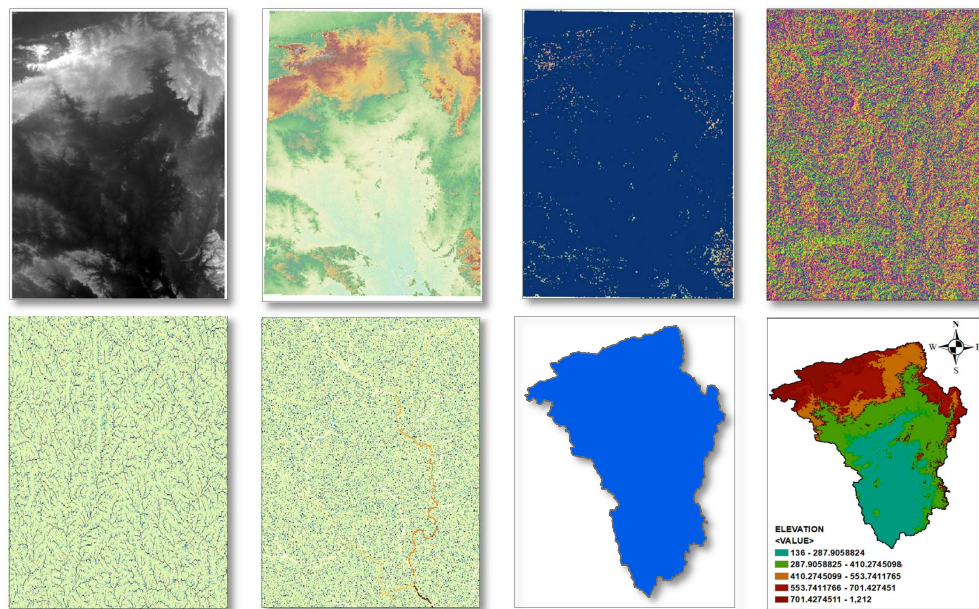


Figure 3 Processing of the DEM into a delineated watershed.

Determination of canopy coverage

Canopy coverage was determined through the MODIS Land Cover - Product MCD12Q1. The tiles were downloaded from earth explorer. Data are distributed by the USGS at 500 m resolution in standard MODIS grid tiles The Land Use Land Cover (LULC) map was derived from the Wainganga Basin map as shown in Figure 4. The resulting canopy fraction was determined to be 0.27.

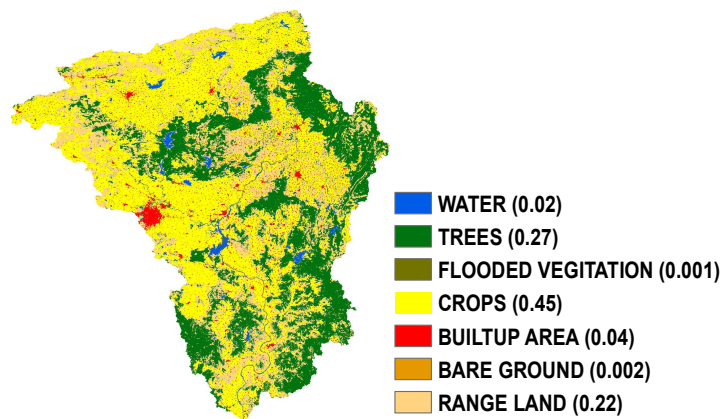


Figure 4 Land use land cover of Wainganga river basin.

Determination of soil parameter

To determine soil hydraulic parameters (Φ_{fc} , Φ_{pc} , Φ_{wp}), on-site measurements of soil depth and saturated hydraulic conductivity are recommended. Alternatively, soil-survey data can be utilized for the estimation of these parameters. The Soil Map of Maharashtra [25], published by the National Bureau of Soil Survey and Land Use Planning (ICAR), was acquired, digitized, and subsequently geo-referenced. The raster image was overlaid with the boundary of the Wainganga basin. Following this, the soil map was categorized into hydrological soil groups. The determination of the range of values for soil hydraulic parameters was based on the soil types within the basin. Figure 5 illustrates the soil map of the Wainganga basin.

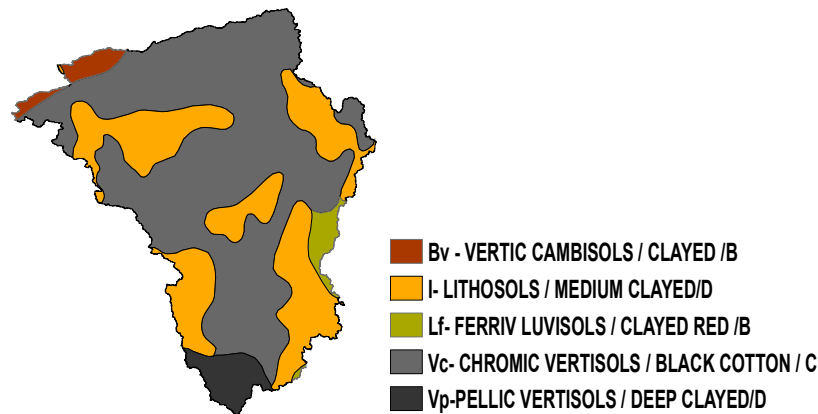


Figure 5 Soil Map of Wainganga basin.

Soil moisture accounting model structure

The conceptual Soil Moisture Accounting (SMA) model utilizes a soil moisture system to consistently track the storage and movement of water through different soil layers. The upper layer signifies surface soil conditions and includes interception storage, while the lower layer represents deeper soil strata and groundwater storage. Within each layer, there are rapid components (free water) primarily influenced by gravitational forces and slow components (tension water) affected by evapotranspiration and diffusion. Consequently, the SMA model, as part of a hydrologic model, extends beyond merely estimating soil moisture; it serves as a comprehensive framework that encompasses surface runoff and evapotranspiration processes.

In instances where precipitation exceeds the capacities for percolation and interflow, the upper zone storage reaches its limit, leading to overflow and the occurrence of overland flow. The Soil Moisture Accounting (SMA) model, comprising a total of 15 parameters, operates as a saturation excess model. The model takes inputs such as Mean Areal Precipitation and Potential Evapotranspiration (PET). When both a canopy and surface method are employed in conjunction with the soil moisture accounting loss method, the system can be conceptualized. [26]. A Monte Carlo simulation is employed to simulate the likelihood of various outcomes in a system where predictions are challenging due to the involvement of random variables to grasp the effects of uncertainty. The SMA model has been implemented in Python, allowing for straightforward execution on a personal computer (PC) and is capable to run 10,000 simulation within 120 - 300 s. This facilitates ease of use and accessibility, making the model accessible to a wide range of users who can run it on their local machines. The model structure can be studied as storage and flow component.

Storage component

Interception model

The model places significant emphasis on the precipitation or rainfall received on the current day as a pivotal factor influencing the potential water interception by vegetation. Equally crucial is the rate of evaporation occurring on the current day. $\text{Intept}_{\text{max}}$ represents the maximum interception capacity measured in millimeters. Within the model, intcept_n denotes the interception depth on the n th day (also in millimeters), while evpt_n signifies the depth of evaporation from the interception store in millimeters. Additionally, rainfall_n represents the depth of rainfall on the n th day, and intstore_n indicates the interception store depth on the n th day, both measured in millimeters.

Section 1;

$$\text{If, } \text{PotET}_n > \text{Intept}_{\text{max}}; \text{ then, } \text{EVP}_{\text{max}} = \text{Intept}_{\text{max}} \text{ Or } \text{PotET}_n < \text{Intept}_{\text{max}}; \text{ then } \text{EVP}_{\text{max}} = \text{PotET}_n \quad (1)$$

Section 2;

If, $0 \leq \text{intstore}_{n-1} \leq \text{Intept}_{\text{max}}$ and, Case (1)

If, $\text{rainfall}_n \leq (\text{Intept}_{\text{max}} - \text{intstore}_{n-1})$

$$\text{Then, } \text{intcept}_n = \text{rainfall}_n \text{ and } \text{evp}_n = \min((\text{intstore}_{n-1} + \text{rainfall}_n), \text{EVP}_{\text{max}}) \quad (2)$$

Case (2)

If, $\text{rainfall}_n \geq (\text{Intept}_{\text{max}} - \text{intstore}_{n-1})$

Then, $\text{Intercept}_n = (\text{Intept}_{\text{max}} - \text{interstore}_{n-1})$ and $\text{evp}_n = \text{EVP}_{\text{max}}$

Section 3;

$$\text{intstore}_n = \text{intstore}_{n-1} + \text{intcept}_n - \text{evp}_n \tag{3}$$

Net rainfall

Net rainfall represents the segment of rainfall that effectively reaches the soil, contributing to soil moisture or runoff, and accounting for losses due to interception. The calculation of net rainfall is determined as follows:

$$\text{rainnet}_n = (\text{rainfall}_n - \text{intcep}_n) * \text{canopy} + \text{rainfall}_n * (1 - \text{canopy}) \tag{4}$$

where, rainnet_n is the net rainfall (mm), on nth day; Canopy refers to the proportion of a catchment area covered by vegetation, often including trees, shrubs, and various plant types.

Modeling direct runoff

1) Basic concepts of the unit hydrograph model

The unit hydrograph is a widely recognized and frequently applied empirical model within the field of hydrology. (S. K. Jain, n.d.) Its primary purpose is to depict the connection between direct runoff. Creating a unit hydrograph for a particular watershed involves scrutinizing historical rainfall and stream flow data (Adeyi *et al.*, 2020).

$$\text{UH}_{\text{depth}} = \sum_{m=1}^{n \leq M} P_m \text{U}_{n-m+1} \tag{5}$$

where Q_n = storm hydrograph ordinate at time $n\Delta t$;

P_m = rainfall excess depth in time interval $m\Delta t$ to $(m+1)\Delta t$;

M = total number of discrete rainfall pulses; and

U_{n-m+1} = UH ordinate at time $(n-m+1)\Delta t$.

Q_n and P_m are flow rate and depth and U_{n-m+1} has dimensions of flow rate per unit depth.

2) SCS Unit hydrograph model

The model under consideration incorporates a UH (Unit Hydrograph) Model that relies on parametric principles. This UH model is formulated based on the recommendations of the Soil Conservation Service (SCS), utilizing averages derived from observed data collected across numerous small agricultural watersheds throughout the United States.

3) SCS Triangular unit hydrograph

Graph 1, a curvilinear unit hydrograph is illustrated, where (Q/Q_p) serves as the UH ordinate, representing discharge (Q) expressed as a ratio to peak discharge. The abscissa is denoted by (t/T_p) , representing time (t) expressed as a ratio to the time to peak (T_p).

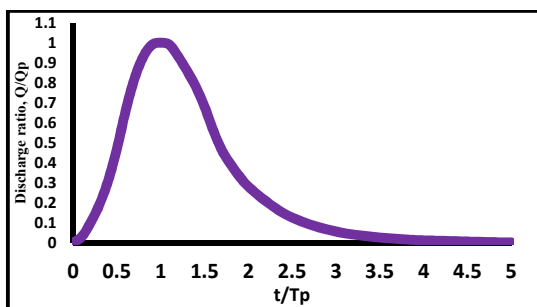
$$\frac{Q}{Q_p} = 1 \quad \text{When,} \quad \frac{t}{T_p} = 1$$

Below **Table 1** indicates coordinates of SCS dimensionless unit hydrograph.

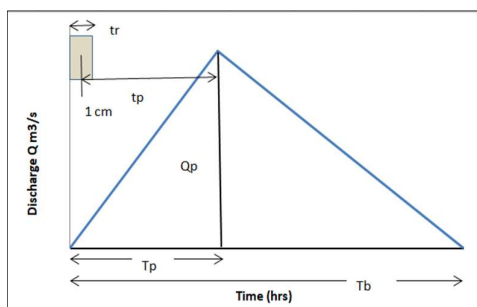
Table 1 Coordinates of SCS dimensionless unit hydrograph.

Time ratio (t/T_p)	Discharge ratio (Q/Q_p)	Time ratio (t/T_p)	Discharge ratio (Q/Q_p)	Time ratio (t/T_p)	Discharge ratio (Q/Q_p)
0	0	1.1	0.99	2.4	0.147
0.1	0.03	1.2	0.93	2.6	0.107
0.2	0.1	1.3	0.86	2.8	0.077
0.3	0.19	1.4	0.78	3	0.055
0.4	0.31	1.5	0.68	3.2	0.04

Time ratio (t/T _p)	Discharge ratio (Q/Q _p)	Time ratio (t/T _p)	Discharge ratio (Q/Q _p)	Time ratio (t/T _p)	Discharge ratio (Q/Q _p)
0.5	0.47	1.6	0.56	3.4	0.029
0.6	0.66	1.7	0.46	3.6	0.021
0.7	0.82	1.8	0.39	3.8	0.015
0.8	0.93	1.9	0.33	4	0.011
0.9	0.99	2	0.28	4.5	0.005
1	1	2.2	0.207	5	0



Graph 1: SCS Unit Hydrograph



Graph 2: SCS Unit triangular hydrograph

From Graph 2,
 Q_p = peak discharge in m³/s
 t_r = duration of effective rainfall
 T_p = time of rise or time to peak
 = (t_r/2) + t_p
 t_p = lag time
 T_b = base length (base Time)
 SCS suggests that the time of recession; (T_b - T_p) = 1.67 T_p
 Thus; T_b = 2.67 T_p

Since the area under the unit hydrograph is Equivalent to 1 cm, If A = area of the watershed in km²

$$\frac{1}{2} Q_p \times (2.67 T_p) \times (3,600) = \frac{1}{100} \times A \times 10^4$$

$$Q_p = \frac{2A \times 10^4}{3600(2.67 T_p)} \text{ for 1 cm rainfall depth}$$

$$Q_p = \frac{2.08 A}{T_p} \tag{10}$$

Further on the basis of a large number of small rural watersheds, SCS found that;

$$t_p = 0.6 t_c$$

where , t_c = time of concentration , which is defined as the time taken for a drop of water from the farthest part of the catchment to reach the outlet.

The SCS model, in SI unit, used to calculate t_c is;

$$t_c = \frac{227 L^{0.8} (\lambda+1)^{0.7}}{10^5 \sqrt{S}} \tag{11}$$

t_c in hr, in which;

L = length of divide (m),

S = average watershed slope (in percent %)

Λ = curve number function, which is defined as the Potential Maximum

Retention and expressed as;

$$\lambda = \frac{1000}{CN} - 10 \quad (12)$$

CN = Curve number for deferent soil/landuse.

Thus;

$$T_p = \frac{t_r}{2} + 0.6t_c \quad (13)$$

$$T_r = \frac{2}{15}t_c \quad (14)$$

$$T_p = \frac{2}{3}t_c \quad (15)$$

$$T_b = \frac{8}{3}t_p \quad (16)$$

The SCS triangular unit hydrograph is a popular method used in watershed development activities, especially in small watersheds (Dang & Kumar, 2017). To use the SCS UH, one needs to determine only 2 things:

- 1) Time to peak, T_p (hr)
- 2) Peak discharge, Q_p (m^3/s)

Flow component

The model employed for simulating water movement within a watershed or catchment area dictates the flow into, out of, and within various storage volumes. This flow can manifest in different forms, including:

- 1) Precipitation

Precipitation serves as an external water source that enters the hydrological system and undergoes storage, transport, or other processes within diverse components like soil moisture, groundwater, and surface runoff. As precipitation occurs, a segment of it is intercepted by vegetation, including leaves, branches, and plant stems. Once the canopy interception storage is filled with precipitation, any surplus water becomes available for infiltration into the soil.

- 2) Infiltration model

Following the filling of the canopy interception storage by precipitation (if it occurs), any excess water becomes accessible for infiltration into the soil. The model calculates the potential evaporation infiltration volume as follows:

$$P_{infil} = Infil_{max} * \left(1 - \frac{\Phi SW}{\Phi_{fc}}\right) \quad (17)$$

where, Infil = potential evaporation infiltration volume

$Infil_{max}$ = maximum infiltration rate

ΦSW = volume in the soil storage at the beginning of the time step

Φ_{fc} = maximum volume of the soil storage

Act_{infil} represents the actual infiltration volume during a specific time interval. The actual infiltration, Act_{infil} , is determined as the minimum of 2 factors that is P_{infil} and volume of water available for infiltration ($rain_{net}$).

- 3) Actual evapotranspiration

Part (1);

EVP from interception model given by Eq. (1) (18)

Part (2);

Case (1) if, $\Phi_{wp} \leq \Phi SW_n < \Phi_{fc}$ EVP from Eq. (2)

$$uzet_n = (pet_n - evp_n) * \left[\frac{(\Phi SW_n - \Phi_{wp})}{\Phi_{fc}}\right] \left(1 - \frac{(\Phi SW_n - \Phi_{wp})}{\Phi_{fc}}\right) lzetn = (petn - evpn - uzetn)e^{-(\Lambda+1)} \quad (19)$$

Case (2) if, $\Phi_{fc} \leq \Phi_{sw_n}$ EVP from Eq. (2);

$$U_{zetn} = (petn - evpn) \quad lz_{etn} = (petn - evpn - uz_{etn}) * e^{-\Lambda} \quad (20)$$

Part (3);

$$a_{etn} = evp_n + uz_{etn} + lz_{etn} \quad (21)$$

where, A_{et} = Actual evapotranspiration (mm)

uz_{etn} = Upper soil zone evapotranspiration (mm),

lz_{etn} = Evapotranspiration (mm) from ground water store;

Λ = constant governing evapotranspiration from lower zone (parameter).

4) Soil moisture storage

Applying a mass balance equation at each time step is a fundamental and common approach. Soil moisture content is modified by following equation.

$$\Phi_{sw_n} = \Phi_{sw_{n-1}} + rain_{etn} (1 - U_{H_{Depth}}) - uz_{etn} - p_{flow_{n-1}} - drain_{n-1} - sz_{ro_{n-1}} \quad (22)$$

$$\Phi_{sw_n} = \Phi_{sw_{n-1}} - uz_{etn} - p_{flow_{n-1}} - drain_{n-1} - sz_{ro_{n-1}} \quad (23)$$

where,

Φ_{sw_n} = soil zone water content (mm),

$\Phi_{sw_{1n}}$ = Previous day soil zone water content after losses (mm),

$\Phi_{sw_{n-1}}$ = Previous day soil zone water content (mm),

uz_{etn} = Previous day evapotranspiration from upper soil zone in mm,

$p_{flow_{n-1}}$ = Macropore flow in mm,

$drain_{n-1}$ = Drainage in mm,

$\Phi_{sz_{ro_{n-1}}}$ = Interflow in mm.

5) Inter flow

Interflow denotes the subsurface lateral movement of water through the soil profile situated above the groundwater table but below the surface. This phenomenon typically arises when the soil reaches saturation, impeding further infiltration of water into the soil. The model employs a simplification by assuming a linear relationship between soil moisture properties, such as soil moisture content (Φ_{SW} - Soil Zone Water Content), field capacity (Φ_{FC}), and wilting point (Φ_{WP}), to determine interflow. The model posits that the maximum potential for interflow happens when the soil is saturated ($\Phi_{SW} = \text{field capacity} - \Phi_{WP}$). The model allows for interflow to persist until the soil moisture content exceeds field capacity.

$$\Phi_{sz_{ro}} = \text{MaxSoil Infil} \left(\frac{\Phi_{SW}}{\Phi_{pc}} \right) \left(1 - \frac{\Phi_{GW}}{\Phi_{GW_{max}}} \right) \quad (24)$$

6) Base flow

The groundwater store, or aquifer, undergoes recharge from excess water that infiltrates beyond the field capacity of the soil. Base flow, a component of streamflow sustained by groundwater discharge during dry periods with minimal or no direct runoff from precipitation, represents the consistent, gradual input of groundwater to streams or rivers, ensuring flow continuity even in droughts or dry spells. Mathematically, the determination of base flow is expressed as follows:

$$\theta_{gw_{ro}} = \text{Maxsoilper} * \left(\frac{\Phi_{gw}}{\Phi_{gw_{max}}} \right) * \left(1 - \frac{\Phi_{gw_n}}{\Phi_{gw_{max}}} \right) \quad (25)$$

Inflow to ground water store is drainage from upper soil layer. Out flow is mainly base flow and lower zone evapotranspiration. For daily updating of ground water store following equation is used;

$$\Phi_{gw_n} = \Phi_{gw_{n-1}} + drain - lz_{etn} - gw_{ro_{n-1}} - \text{infil} \quad (26)$$

where gw_{ro_n} is ground water runoff in mm, Φ_{GW_n} is the ground water store in mm.

7) Muskingum model

The fundamental idea behind the Muskingum model is to approximate the solution to the continuity equation for flow routing by employing a finite difference approximation.

$$\left(\frac{I_{t-1}+I_t}{2}\right) - \left(\frac{O_{t-1}+O_t}{2}\right) = \left(\frac{S_t-S_{t-1}}{\Delta t}\right) \quad (27)$$

The utilization of prism storage and wedge storage is a prevalent practice in hydraulic and hydrological modeling for depicting storage volume in a river reach during flood events. This methodology aids in assessing the overall storage capacity of a river reach and its fluctuations under different flow conditions.

1) Prism storage: Prism storage denotes the volume of water retained within a reach under steady flow conditions, typically aligning with base flow scenarios.

2) Wedge storage: Wedge storage represents the supplementary storage volume occurring during unsteady flow conditions, such as during the rising and falling stages of a flood. These principles aid in evaluating the responses of river reaches to different flow conditions and in estimating how floodwaters are stored and released as they traverse the reach.

Figure 6 provides additional clarity on the principles of prism storage and wedge storage. This understanding is pivotal for accurate flood assessments and efficient floodplain management practices.

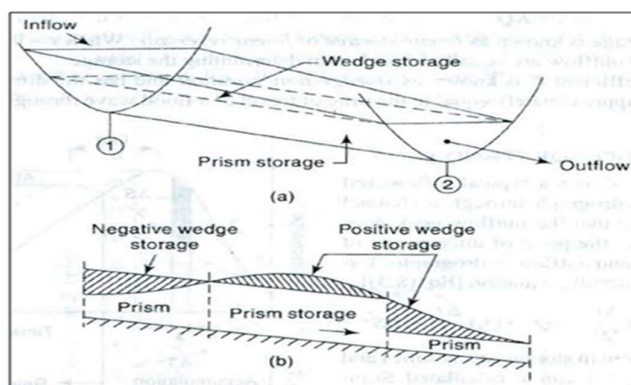


Figure 6 Prism and Wedge storage.

The formula provided, $V = O * K$, represents a fundamental equation connecting the volume of water storage (V), the outflow rate (O), and the travel time through the reach (K). The expression $V = (I - O) * K$ mathematically represents the volume of water storage (V) in the wedge-shaped region. The travel time (K) is crucial in considering the duration it takes for this change in volume to transpire. Therefore, according to the Muskingum model, the storage is defined as:

$$\begin{aligned} S_t &= KO_t + KX(I_t - O_t) \\ &= K [XI_t + (1-X) O_t] \end{aligned} \quad (28)$$

S_t = Storage
 K = Travel Time
 X = dimensionless weight ($0 \leq X \leq 0.5$)

From above equation the quantity $[XI_t + (1-X) O_t]$ is weighted discharge. If Eq. (27) is substituted into Eq. (28) and the result is rearranged to isolate the unknown values at time t , the result is:

$$O_t = \left(\frac{\Delta t - 2KX}{2K(1-X) + \Delta t}\right) * I_t + \left(\frac{\Delta t + 2KX}{2K(1-X) + \Delta t}\right) * I_{t-1} + \left(\frac{2K(1-K) - \Delta t}{2K(1-X) + \Delta t}\right) O_{t-1} \quad (29)$$

The model inputs above equation to determine discharge ordinates of hydrograph provided time stepped rainfall, initial condition ($O_t = 0$) and muskingum parameter K and X respectively.

Performance indicator

1) NSE (Nash-Sutcliffe Efficiency)

Stands as a widely acknowledged and frequently employed metric for evaluating hydrological models. [29] Its purpose is to evaluate the quality of fit by measuring the agreement between simulated values (S) and observed values (O) of a hydrological variable, typically stream flow.

$$NSE = 1 - \frac{\sum(Q_{i,s} - Q_{i,o})^2}{\sum(Q_{i,o} - Q_o)^2} \quad (30)$$

NSE = Nash Sutcliff efficiency

$Q_{i,s}$ = is the ith simulated discharge

$Q_{i,o}$ = is the ith observed discharge

2) Sum of Squared Errors (SSE)

$$SSE = \sum_{i=1}^n (Q_{i,s} - Q_{i,o})^2 \quad (31)$$

3) Sum of Squared Log Errors (SLE)

$$SLE = \sum_{i=1}^n \{\log(Q_{i,s}) - \log(Q_{i,o})\}^2 \quad (32)$$

4) Sum of Absolute Errors (SAE)

$$SAE = \sum_{i=1}^n |Q_{i,s} - Q_{i,o}| \quad (33)$$

SME Model software development

A user-friendly software package for Windows is developed using Python. The software requires input files containing precipitation, evapotranspiration, and river flow data. Within the software package's main interface, users have the option to manually modify model parameter values. Upon model's validity for the period from 2001 to 2017. The model provides a comprehensive overview of the model's performance throughout the calibration period from 2001 to 2010 and the validation period from 2011 to 2017. Additionally, the software package incorporates a Monte Carlo simulation option, allowing users to vary model parameters within specified ranges and obtain results for a user-defined number of realizations. Utilizing Monte Carlo simulations, the optimal parameter set can be determined [30]. **Figure 7** is output of model indicating simulated and observed discharge.

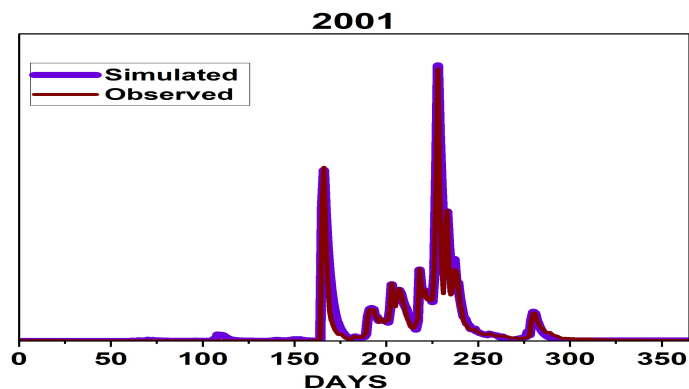


Figure 7 Simulated vs. observed discharge.

Software Availability:

Name of Software: SME Model

Program Language: Python

Hardware required: PC/Mac

Note: SME MODEL is registered at Copyrights of India.

Parameter optimization, Sensitivity and Uncertainty analysis of model parameter

Parameter optimization

Models often involve numerous parameters, and identifying the optimal combination of these parameters can be approached as a search problem [31]. The calibration process typically entails a trial-and-error method, adjusting parameter values to align the model’s input-output behavior with the real-world system it represents. The model calibration phase spans from 2001 to 2010, followed by a validation phase from 2011 to 2017. The steps in calibration are:

- 1) Commence by establishing an objective function or fitness function, which quantifies the degree of fit between model predictions and observed data.
- 2) Specify the input parameters for the model (Φ_{GW} , Φ_{SW} , K , X , Φ_{fc} , Φ_{pc}).
- 3) Define the range and probability distribution for parameter.
- 4) Input each set of parameter values into the model and execute simulations. Generate a set of 10 thousand sample parameter sets with random values.
- 5) Calculate performance indices (NSE, SSE, SLE, SAE) after running the model for each calibrated year, noting the parameter set with the maximum efficiency.
- 6) Obtain the optimal parameter set by computing the average value that represents the highest efficiency over the calibration period.

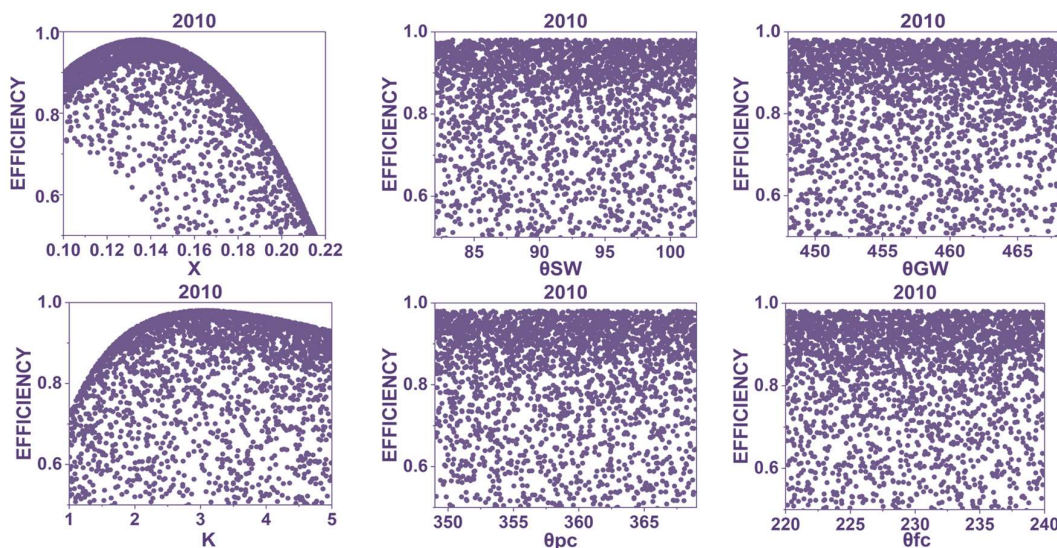
Sensitivity analysis

Estimation of Sensitivity

In the SME model, conducting sensitivity analysis serves the primary purpose of examining the sensitivity of simulated runoff to parameters influencing runoff generation [32,33]. The specific focus is on understanding how these parameters vary with changes in soil, vegetation, and other conditions. Likelihood values for each parameter set were calculated, and a scatter plot of the Nash-Sutcliffe efficiency coefficient was generated against each parameter [34,35]. Graph 3 illustrates depicts the relationship between parameters and efficiency which is output of Monte Carlo simulation given by SMA model.

It can be observed that the parameters are divided into 2 categories.

- 1) Insensitive parameters: It can be observed that the parameters Φ_{GW} , Φ_{SW} , Φ_{fc} , Φ_{pc} are not sensitive. The characteristic of these parameters is that the data scatter evenly and without obvious trend, which demonstrates that the different values of this parameter have less impact on the simulation result.
- 2) Sensitive parameters: The changes of parameters X and K have a greater influence on the simulation results.

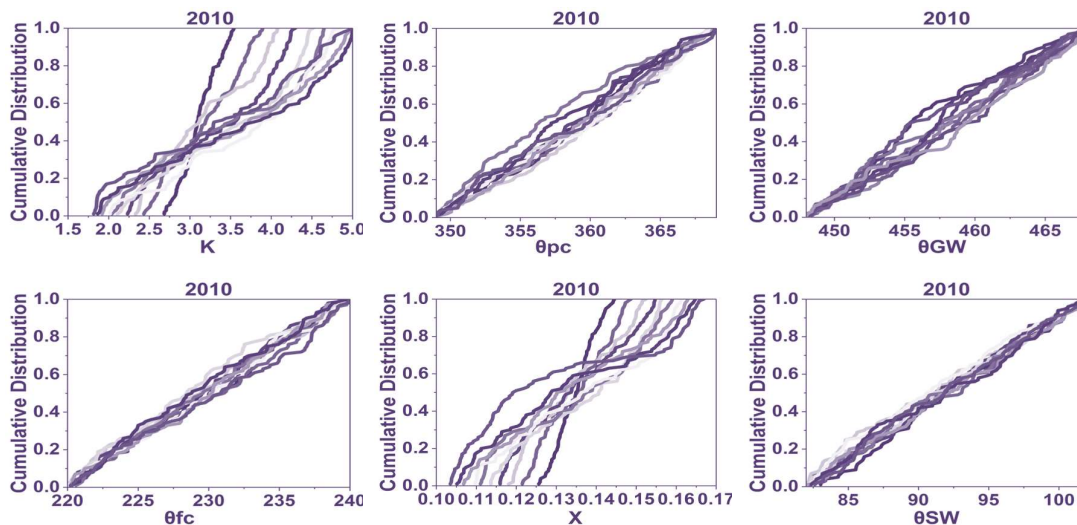


Graph 3: Monte Carlo simulation Dotty plots.

Sensitivity analysis plot

The parameter sensitivity plots in graph 4 illustrate the cumulative distributions that is efficiency of parameter values grouped based on the ranking of each Monte Carlo run for a particular likelihood

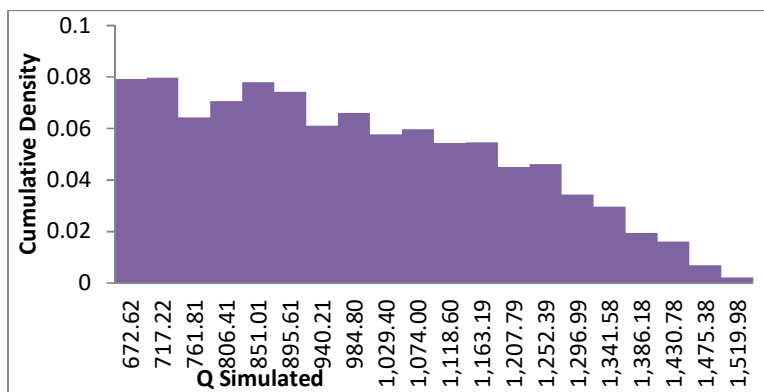
measure or predicted variable [36]. It is output of Monte Carlo simulation given by SMA model. Significant disparities between the cumulative distributions for a given likelihood measure or variable indicate sensitivity to that parameter. Each panel displays 10 curves, each corresponding to a single bin. In general, an insensitive parameter will yield a straight one-to-one line, while a sensitive model parameter will exhibit differences in separation and form among the cumulative frequency distribution curves.



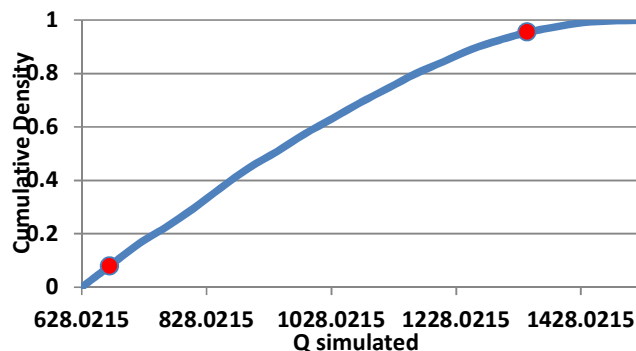
Graph 4: Sensitivity plots

Uncertainty estimation

Enhancements in the quality and accessibility of data, coupled with advancements in hydrological process simulations, are poised to bolster forecast capabilities [37,38]. Subsequently, likelihood values are computed based on a predefined likelihood measure (i.e., a metric assessing goodness of fit) to assess the level of correspondence between each simulation and the observed behavior of the system.



Graph 5(a): Histogram of predicted variable (Qsim)



Graph 5(b): Cumulative distribution of a simulated discharge

In this investigation, the Nash-Sutcliffe Efficiency (NSE) is employed as the likelihood measure. Graph 5(a) illustrates histograms and cumulative distribution plots of a simulated discharge, with weighting based on the likelihood measure. Additionally, Graph 5(b) displays the 5th and 95th percentile sample quantiles, denoted as red dots, on the cumulative distribution plot.

Conclusions

The Soil Moisture Accounting model, when combined with GIS techniques, demonstrates a strong alignment with observed and simulated stream flow. When integrated with the Monte Carlo algorithm, it reveals that the model employed in this study adheres to the principles of equifinality and non-uniqueness. In essence, this implies that when fitting the model to real-world data, there are numerous sets of model parameters that can be used, and each of these parameter sets can yield a satisfactory match with the observed data. This practical insight suggests that the system being modeled is intricate, and there exists inherent uncertainty in determining the “correct” model parameters, as multiple sets of parameters can yield comparable results. The optimum parameter values, which lead to favorable model performance, closely resemble previously identified optima. A sensitivity analysis underscores that the Muskingum constants K and X exert a significant influence on the model’s performance, while the parameters Φ_{GW} , Φ_{SW} , K , X , Φ_{fc} , and Φ_{qc} have a relatively minor impact on the model’s functionality. In the realm of uncertainty analysis, one can determine confidence intervals (e.g., 95 and 5 % intervals) surrounding the outcome of interest by utilizing the results from the Monte Carlo Simulation. These intervals serve as a measure of the precision and reliability of the estimate. The model has shown promise in its initial application, indicating its effectiveness in some aspect, potentially in its ability to model or analyze a specific system or process.

Acknowledgment

I am thankful to Dr. Rajesh Kherde for support. I am extremely grateful to USGS, Copernicus Climate Change Data Store, India WRIS and IMD Pune and HDUG Nashik for providing data.

References

- [1] ZK Tesemma, Y Wei, MC Peel and AW Western. The effect of year-to-year variability of leaf area index on Variable Infiltration Capacity model performance and simulation of runoff. *Adv. Water Resour.* 2015; **83**, 310-22.
- [2] K Wang, H Shi, J Chen and T Li. An improved operation-based reservoir scheme integrated with Variable Infiltration Capacity model for multiyear and multipurpose reservoirs. *J. Hydrol.* 2019; **571**, 365-75.
- [3] K Bhardwaj, D Shah, S Aadhar and V Mishra. Propagation of meteorological to hydrological droughts in India. *J. Geophys. Res. Atmos.* 2020; **125**, e2020JD033455.
- [4] A Zalnezhad, A Rahman, F Ahamed and M Vafakhah. Design flood estimation at ungauged catchments using index flood method and quantile regression technique: A case study for South East Australia. *Nat. Hazards* 2023; **119**, 1839-62.
- [5] A Shokri. Development of a new Event-Based Rainfall-Runoff equation based on average rainfall intensity during an event. *Environ. Model. Assess.* 2023; **28**, 651-64.
- [6] L Wen, CA Lin, Z Wu, G Lu, J Pomeroy and Y Zhu. Reconstructing sixty year (1950-2009) daily

- soil moisture over the Canadian prairies using the variable infiltration capacity model. *Can. Water Resour. J.* 2011; **36**, 83-102.
- [7] S Koneti, SL Sunkara and PS Roy. Hydrological modeling with respect to impact of land-use and land-cover change on the runoff dynamics in Godavari river basin using the HEC-HMS model. *ISPRS Int. J. Geo Inform.* 2018; **7**, 206.
- [8] C Birkel and AC Barahona. *Rainfall-Runoff modeling: A brief overview*. Elsevier, Amsterdam, Netherlands, 2017.
- [9] A Srivastava, N Kumari and M Maza. Hydrological response to agricultural land use heterogeneity using variable infiltration capacity model. *Water Resour. Manag.* 2020; **34**, 3779-94.
- [10] R Singh, KK Garg, SP Wani, RK Tewari and SK Dhyani. Impact of water management interventions on hydrology and ecosystem services in Garhkundar-Dabar watershed of Bundelkhand region, Central India. *J. Hydrol.* 2014; **509**, 132-49.
- [11] A Adeogun, B Sule, A Salami and O Okeola. GIS-Based hydrological modelling using swat: Case study of upstream watershed of jebba reservoir in Nigeria. *Niger. J. Tech.* 2014; **33**, 351.
- [12] D Halwatura and MMM Najim. Application of the HEC-HMS model for runoff simulation in a tropical catchment. *Environ. Model. Software* 2013; **46**, 155-62.
- [13] M Smaranika, MK Jha, S Biswal and D Sena. Assessing variability of infiltration characteristics and reliability of infiltration models in a tropical Sub-humid region of India. *Sci. Rep.* 2020; **10**, 1515.
- [14] Rohtash, LN Thakural, MK Choudhary and D Tiwari. Rainfall runoff modeling using SWAT model for Chaliyr Basin Kerala, India. *Int. J. Sci. Res.* 2018; **8**, 90-7.
- [15] R Horan, R Gowri, PS Wable, H Baron, VDJ Keller, KK Garg, PP Mujumdar, H Houghton-Carr and G Rees. A comparative assessment of hydrological models in the upper cauvery catchment. *Water* 2021; **13**, 151.
- [16] P Darbandsari and P Coulibaly. Inter-comparison of lumped hydrological models in data-scarce watersheds using different precipitation forcing data sets: Case study of Northern Ontario, Canada. *J. Hydrol. Reg. Stud.* 2020; **31**, 100730.
- [17] MK Jain, UC Kothiyari and KGR Raju. A GIS based distributed rainfall-runoff model. *J. Hydrol.* 2004; **299**, 107-35.
- [18] LT Arantes, ACP Carvalho, APP Carvalho, R Lorandi, LE Moschini and JAD Lollo. Surface runoff associated with climate change and land use and land cover in southeast region of Brazil. *Environ. Challenges* 2021; **3**, 100054.
- [19] D Sun, H Yang, D Guan, M Yang, J Wu, F Yuan, C Jin, A Wang and Y Zhang. The effects of land use change on soil infiltration capacity in China: A meta-analysis. *Sci. Total Environ.* 2018; **626**, 1394-401.
- [20] V Garg, IR Dhuma, BR Nikam1, PK Thakur, SP Aggarwal, SK Srivastav and AS Kumar. Water resources assessment of godavari river basin, India, Available at: https://www.researchgate.net/publication/314370194_WATER_RESOURCES_ASSESSMENT_OF_GODAVARI_RIVER_BASIN_INDIA, accessed January 2016.
- [21] A Kunnath-Poovakka and TI Eldho. A comparative study of conceptual rainfall-runoff models GR4J, AWBM and Sacramento at catchments in the upper Godavari river basin, India. *J. Earth Syst. Sci.* 2019; **128**, 33.
- [22] X Yan, B Lin, X Chen, H Yao, W Ruan and L Xiaocheng. Impacts of small and medium-sized reservoirs on streamflow in two basins of Southeast China, using a hydrological model to separate influences of multiple drivers. *J. Hydrol. Reg. Stud.* 2023; **50**, 101582.
- [23] JO Oleyiblo and L Zhi-Jia. Application of HEC-HMS for flood forecasting in Misai and Wan'an catchments in China. *Water Sci. Eng.* 2010; **3**, 14-22.
- [24] F Hussain, W Ray-Shyan and Y Kaichun. Application of physically based Semi-Distributed Hec-Hms model for flow simulation in tributary catchments of Kaohsiung Area Taiwan. *J. Mar. Sci. Tech.* 2021; **29**, 42-62.
- [25] Finance Division, Ministry of Finance Government of the People's Republic of Bangladesh. *Gender budget report 2023-24*. Finance Division, Ministry of Finance Government of the People's Republic of Bangladesh, Bangladesh, 2023.
- [26] E Abushandi. Modelling rainfall runoff relations using HEC-HMS and IHACRES for a single rain event in an arid region of Jordan. *Water Resour. Manag.* 2014; **27**, 2391-409.
- [27] GO Adeyi, AI Adigun, NC Onyeocha and OC Okeke. Unit hydrograph: Concepts, estimation methods and applications in hydrological sciences. *IJESC* 2020; **10**, 26211-7.
- [28] ATN Dang and L Kumar. Application of remote sensing and GIS-based hydrological modelling for flood risk analysis: A case study of District 8, Ho Chi Minh city, Vietnam. *Geomatics Nat. Hazards*

- Risk* 2017; **8**, 1792-811.
- [29] T Razavi and P Coulibaly. An evaluation of regionalization and watershed classification schemes for continuous daily streamflow prediction in ungauged watersheds. *Can. Water Resour. J.* 2017; **42**, 2-20.
- [30] EA Oduntan, JO Iyaniwura and EO Amoo. A Monte Carlo simulation framework on the relative performance of system estimators in the presence of multicollinearity. *Cogent Soc. Sci.* 2021; **7**, 1926071.
- [31] D Basin, T Jiang, Y David, C Xu, X Chen, VP Singh and X Chen. Comparison of hydrological impacts of climate change simulated by six hydrological models in the Dongjiang Basin, South China. *J. Hydrol.* 2007; **336**, 316-33.
- [32] R Lillhare, S Pokorny, SJ Déry, TA Stadnyk and KA Koenig. Sensitivity analysis and uncertainty assessment in water budgets simulated by the variable infiltration capacity model for Canadian subarctic watersheds. *Hydrolog. Process.* 2020; **34**, 2057-75.
- [33] S Naha, MA Rico-Ramirez and R Rosolem. Quantifying the impact of land cover changes on hydrological extremes in India. *Hydrol. Earth Syst. Sci. Discuss.* 2020; **25**, 6339-57.
- [34] CM Rao and A Bardhan. Uncertainties and nonstationarity in streamflow projections under climate change scenarios and the ensuing adaptation strategies in Subarnarekha river basin, India. *Global NEST J.* 2021; **22**, 320-35.
- [35] B Pang, R He and L Zhang. Parameter estimation and uncertainty analysis of the variable infiltration capacity model in the Xitiaoxi catchment. In: Proceedings of the ICFM6 - International Conference on Flood Management, São Paulo, Brazil. 2014, p. 1-8.
- [36] EM Demaria, B Nijssen and T Wagener. Monte carlo sensitivity analysis of land surface parameters using the variable infiltration capacity model. *J. Geophys. Res. Atmos.* 2007; **112**, D11113.
- [37] D Raje and R Krishnan. Bayesian parameter uncertainty modeling in a macroscale hydrologic model and its impact on Indian river basin hydrology under climate change. *Water Resour. Res.* 2012; **48**, W08522.
- [38] TT Zin, M Lu and T Ogura. Assessing recession constant sensitivity and its interaction with data adjustment parameters in continuous hydrological modeling in data scarce basins: A case study using the Xinanjiang model. *Water* 2024; **16**, 286.